Wake structures of two spheres in tandem arrangement at various gaps for $Re = 300$ *

ZOU Jianfeng **, REN Anlu, DENG Jian and CHEN Wenqu

(Department of Mechanics, Zhejiang University, Hangzhou 310027, China)

Received May 28, 2004; revised September 23, 2004

Abstract The virtual boundary method is extended to a 3D application and used to simulate the flow field of two spheres in tandem arrangement for a Reynolds number of 300. The wake structures and flow spectra at various gaps are investigated. The numerical results show that for small gaps ($\approx$1.5), due to the mutual suppress between the wakes of the two spheres, the full flow field is stable and axisymmetric. As the gap is increased to 2.0, an asymmetric but stable flow is constructed through a certain bifurcation. The downstream wake structure is characterized by a double-thread vortex structure that comprises two slender parallel vortex tubes. The double-thread structure has a planar symmetry at gap 2.0. The hairpin-shape vortices are periodically shed from the downstream sphere at gap 2.5, but the planar symmetry persists. The vortex structures at gaps ranging from 3.0 to 4.0 are irregular and the flow field is undergoing a kind of 3D transition. It is up to the large gap 5.0 that the hairpin-shape structures are reconstructed behind the upstream and the downstream sphere, and the planar symmetry is resumed. All these numerical computations were performed on an SGI Origin3900 machine at the Center for Engineering and Scientific Computation of Zhejiang University.

Keywords: virtual boundary method, flow past two spheres, wake structure, flow spectra.

The flow around a sphere is a fundamental problem of fluid dynamics. Although the sphere is the simplest geometry, a number of natural and engineering applications exist such as air pollution, combustion system and chemical processes.

Some valuable results of flow past a single sphere, especially the transitions between different flow regimes, have been achieved experimentally[1—3]. Flow around a single sphere in a uniform flow separates from the surface to form a stable and axisymmetric toroidal vortex at Reynolds number $Re = 24$, where Re is defined in terms of the uniform flow velocity and the diameter of the sphere. The stable flow changes to an asymmetric stable flow through a bifurcation at $Re \approx 210$. A new unstable oscillating flow is formed at $Re > 270$ and the hairpin-shape vortices are periodically shed from the sphere. In the 1990s, a number of numerical simulations for flow past a single sphere were performed. But being restricted by the speed of CPU, storage capacity and algorithm, the axisymmetry assumption incorrect for $Re > 210$ was made in most simulations. The primitive 3D unsteady Navier-Stokes equations were solved by Johnson[4] and Lee[5] to simulate the flow past a single sphere, and their results compared well with previous experimental observations.

Little work has been performed to study the interactions of the wakes of two spheres in tandem or side-by-side arrangement. In the early 1980s, some qualitative experimental results for flow past two spheres were achieved by Yutaka[6]. The latest experimental study on wakes of two spheres placed side by side was carried out by Schouveiler[7] and distinctly different regimes of interactions were observed, depending on the gap between two spheres.

Due to the difficulty in grid generation for the multiply-connected domain of flow past two spheres, no numerical method based on finite difference has been reported. To avoid this difficulty, for flow past two spheres placed side by side at low Reynolds numbers, symmetry was assumed and the physical domain was reduced to one quarter of an ellipsoid-like computational field by Kim[8]. Thus, the calculation was performed on a simply connected domain containing only one quarter of a single sphere, and the dependence of the force on sphere surfaces and the vortex structure on the gap was investigated.

In this paper, the virtual boundary method first

* Supported by National Natural Science Foundation of China (Grant No. 10272094)

** To whom correspondence should be addressed. E-mail: luckyluke@zju.edu.cn

presented by Goldstein[9] has been modified slightly and extended to a 3D application. The currently modified and extended virtual boundary method (called virtual body method here) is then used to study the interaction between the upstream wake and the downstream wake.

1 Virtual body method

The so-called virtual boundary method based on regular meshes was first presented by Goldstein to model a no-slip boundary in flow field. The solid domain is assumed to be filled with fluid and a virtual body-force field is introduced into the Navier-Stokes equations, such that a desired velocity distribution can be assigned to the fluid points on no-slip boundary. The body force field introduced in their work is governed by the following feed-back loop

$$\boldsymbol{F}(\boldsymbol{x}_s, t) = \alpha \int_0^t [\boldsymbol{u}(\boldsymbol{x}_s, \tau) - v(\boldsymbol{x}_s, \tau)]\, d\tau + \beta[\boldsymbol{u}(\boldsymbol{x}_s, t) - v(\boldsymbol{x}_s, t)], \quad (1)$$

where α and β are two negative constants; $\boldsymbol{x}_s$ denotes a boundary point and $\boldsymbol{u}(\boldsymbol{x}_s, t)$ is the fluid velocity at $\boldsymbol{x}_s$; the velocity of the solid boundary point itself is $v(\boldsymbol{x}_s, t)$. Using a pseudo-spectral method, Goldstein applied this procedure to simulate a start up flow around a stationary cylinder.

To well define the no-slip boundary condition, large enough $|\alpha|$ and $|\beta|$ are needed, which makes the governing equations stiff and the stability limit rigid. A Courant-Friedrichs-Lewy number (CFL) with an order of 10^{-3} is used in Goldstein's simulations. The expensive time consumption makes the simulation of flow in complex geometry impossible. Therefore, an alterative expression for the added body-force on no-slip boundary was presented by Fadlun[10],

$$\boldsymbol{F}^{n+1} = -\boldsymbol{RHS}^n + \frac{v^{n+1} - \boldsymbol{u}^n}{\Delta t}, \quad (2)$$

where v^{n+1} is the velocity of solid boundary point at current time level $t+\Delta t$, and $\boldsymbol{u}^n$ is the corresponding fluid velocity at t time level; the term $\boldsymbol{RHS}^n$ contains the convective, viscous and pressure gradient terms in momentum equation at t time level. Thus, at every time level the boundary condition can be defined exactly and no rigid stability limit results from the body-force Eq. (2) introduced into the Navier-Stokes equations.

1.1 Modification of virtual boundary method

The idea of the virtual boundary method was introduced previously. Goldstein and Fadlun imposed the added body-force only at points defining the no-slip boundary; thus unphysical fluid motion was allowed inside the body. But in our study, the added body-force given by Eq. (2) is imposed inside the body as well as on the boundary. With this slight modification the computational efficiency is improved considerably and no numerical flow is allowed inside the body which is especially essential for moving body problem.

1.2 Interpolation procedure

Inside the body, the added body-force can be calculated directly at grid point using the expression given by Eq. (2). A certain interpolation procedure is needed to distribute the added body-force on the curved surface to the grid points nearby. Detailed description is given as follows (Fig. 1): $p_f(x_f, y_f, z_f)$ is a grid point near the solid surface and $p_s(x_s, y_s, z_s)$ is the surface point lying on the line connecting p_f and the sphere center. The field values of four points (denoted by a, b, c and d) with one grid away from p_s are achieved using the bilinear interpolation scheme, then the body-force $\boldsymbol{F}(x_s, y_s, z_s)$ of p_s can be computed. Since the surface point is not coincident with the grid site, the effect of the body-force $\boldsymbol{F}(x_s, y_s, z_s)$ should be distributed to the nearby grid point p_f using linear interpolation, $\boldsymbol{F}(x_f, y_f, z_f) = (1 - ds/dxyz)\boldsymbol{F}(x_s, y_s, z_s)$. Here $dxyz$ is the diagonal length of grid element and ds is the radial distance between p_s and p_f. It should be noted that the body-force is equal to zero for grid points with condition $ds > dxyz$ satisfied.

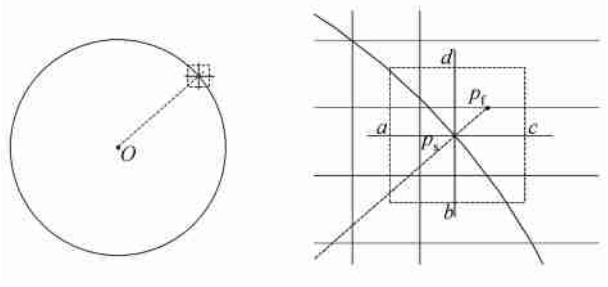

Fig. 1. Body force on surface distributed to meshes near wall.

We call the modified numerical method a virtual body method. In our computation, the Navier-Stokes equations are discretized by finite differences on regular meshes system. It is easy to code and a parallel procedure with high performance is developed. All the simulations here are performed on an SGI Origin3900 machine of the Center for

Engineering and Scientific Computation of Zhejiang University. In the following simulations, the dimensionless spacial increment and time step are set to be 0.05 and 0.005, respectively (i.e. $CFL=0.1$).

2 Solution of governing equations

The non-dimensional Navier-Stokes equations for incompressible viscous flow are written as

$$\nabla \cdot \boldsymbol{V}=0,$$
$$\frac{D\boldsymbol{V}}{Dt}=-\nabla p+\frac{1}{Re}\nabla^2\boldsymbol{V}+\boldsymbol{F}_{\text{add}}, \tag{3}$$

where $\boldsymbol{F}_{\text{add}}=(F_x, F_y, F_z)$ is the added force vector. The diameter D is used as the length scale and the uniform free-stream velocity is the characteristic velocity.

A rectangular computational domain is designed. A free-stream velocity condition is used at the inflow and far field boundaries. A non-reflecting condition is used at the outflow boundary. A pressure Neumann condition is applied to inflow, far field and outflow boundaries and there is no pressure condition needed for the no-slip boundary. The initial flow field is at rest.

We used the Euler-explicit time discretization scheme for convective terms and the second-order-implicit Crank-Nicholson scheme for viscous terms. Spacial derivatives are discretized by second-order central finite difference. Ignore the term of $O(\Delta t^3)$, and the finally obtained algebraic equations system can be solved using generic TDMA algorithm at x and y direction successively.

The pressure variable is solved from the pressure Poisson equation which is derived by applying the divergence operator to the momentum equations. The time dependent term of the pressure Poisson equation is dealt with by Harlow's method[11] and the derivatives are discretized by second-order central difference. To satisfy the compatibility condition, the pressure condition is evaluated at half-grid points near boundary[12, 13].

3 Flow regimes of a single sphere: validation of computational code

To validate the present code, the transitions of wake regimes for flow past a single sphere are investigated. In this paper, the calculated wake structure is visualized using the definition of a vortex as a connected region containing two negative eigenvalues of the $\boldsymbol{S}^2+\Omega^2$ tensor (here $\boldsymbol{S}$ and Ω are respectively the symmetric and antisymmetric parts of the velocity gradient tensor) proposed by Jeong &Hussain[14]. The vortex structures at Reynolds numbers 200, 225, 250 and 275 are listed in Fig. 2, respectively. Two bifurcations are well captured and the two Reynolds numbers of transitions ($200<Re_{c1}<225$, $250<Re_{c2}<275$) are in good agreement with the corresponding experimental results mentioned above. The vortex shedding frequency at $Re=275$ is about 0.123 which compares well with the experimental results of Ref. [3].

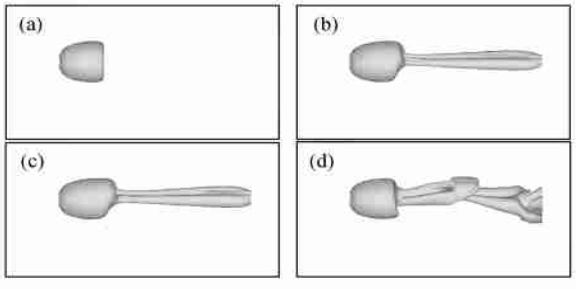

Fig. 2. Vortex structures past a single sphere. (a) $Re=200$; (b) $Re=225$; (c) $Re=250$; (d) $Re=275$.

4 Flow regimes of two spheres system

Figure 3 is the schematic sketch of the flow domain of two spheres with the primary scale parameters, 7.5 D high and 7.5 D wide. The origin of the coordinate system is located at the center of the downstream sphere. A boundary condition with a freestream velocity of $u=1$ is applied at the inlet and outer boundaries. At the outlet, a nonreflecting boundary condition is enforced. The various flow regimes are presented in the following as a function of gap ratio L/D. The same Reynolds number 300 is studied for all the simulations.

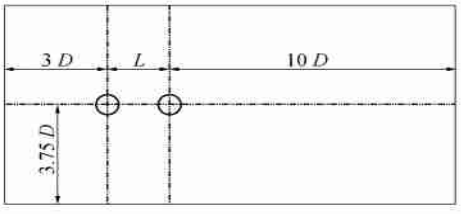

Fig. 3. Scale parameters of the computational domain.

It is known that at $Re=300$ the regular hairpin-shape vortices are periodically shed from the single sphere. From Fig. 4, we find that for small gaps (≈ 1.5), due to the mutual suppress between the wakes of the two spheres, the full flow field is stable and axisymmetric. A vortex ring is confined between

the two spheres.

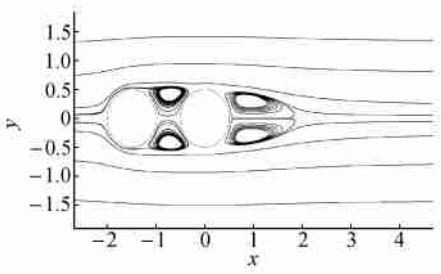

Fig. 4. Streamlines on (x, y) plane for $L/D=1.5$.

At $L/D = 2.0$, the flow is stable but asymmetric. A double-thread vortical structure dragging two slender parallel vortex tubes is observed in the downstream wake (Fig. 5). Suppressed by the downstream sphere, the double-thread structure of the upstream wake cannot be full developed and the rear of the upstream vortex structure is captured by the front part of the downstream sphere.

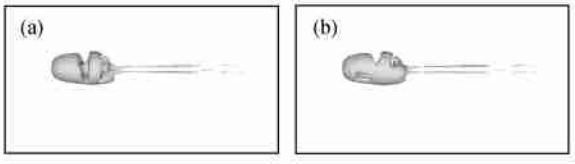

Fig. 5. Wake structure for $L/D=2.0$. (a) x-y view; (b) x-z view.

To understand the transfer property of fluid in the flow field, the paths of several particles originated from either side of, and just out of, the plane which has an angle of -45° with the (x, y) plane near the sphere are shown in Fig. 6. From Fig. 6(a), we know that the flow field is symmetric with respect to the plane mentioned here. In the upstream wake, the upper fluid spirals counterclockwise inward, and then emerges from the center of the upper focus and feeds into the downstream flow field passing through the bottom part of the downstream sphere. The pathline in the downstream wake is similar to that of a single sphere. The lower fluid of the downstream wake spirals counterclockwise inward, and then emerges from the center of the focus and feeds into the center of the upper focus, where it spirals clockwise outward, and eventually passing around the lower focus and joining the downstream flow.

At gap 2.5, an unstable oscillating flow is formed in the flow field and the hairpin-shape vortices are periodically shed from the downstream sphere (Fig. 7). The hairpin structure of the upstream sphere has not been well organized at the present gap 2.5.

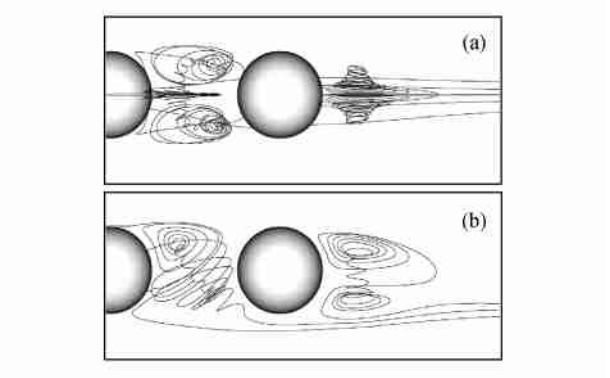

Fig. 6. Particle path near two spheres for $L/D=2.0$. (a) Plane view with an angle 45° from (x, y) plane; (b) Plane view with an angle -45° from (x, y) plane.

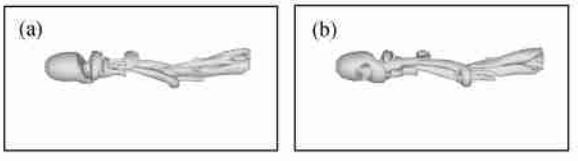

Fig. 7. Wake structure for $L/D=2.5$. (a) x-y view; (b) x-z view.

It is interesting that a plane of symmetry can be found in the unstable flow field (Fig. 8). The position of the plane of symmetry is equal to that of flow field at gap 2.0.

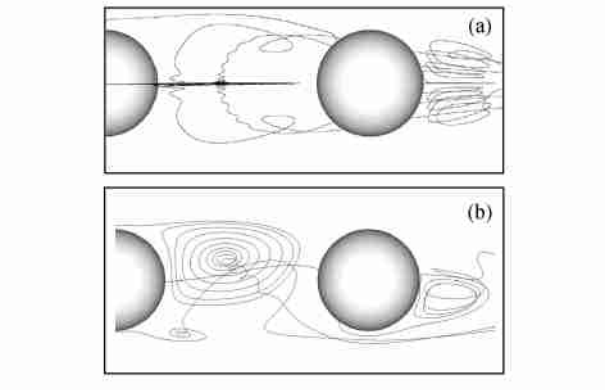

Fig. 8. Streamlines near two spheres for $L/D=2.5$. (a) Plane view with an angle 45° from (x, y) plane; (b) Plane view with an angle -45° from (x, y) plane.

As the gap between two spheres keeps on being increased, an irregular oscillating flow is formed in the wake of the upstream sphere (Fig. 9). A spiral-shape vortex structure extending to the outlet along the centerline can be clearly found in the downstream wake and the flow field is not plane-symmetric any more.

The gap 4.0 is so large that a single loop of hairpin-shape structure is formed between two spheres (Fig. 10). Due to the effect of

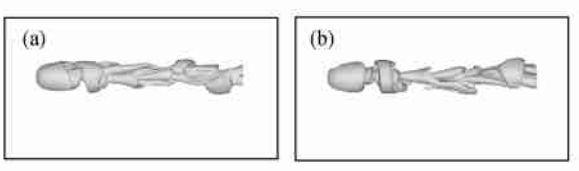

Fig. 9. Wake structure for $L/D=3.0$. (a) x-y view; (b) x-z view.

synchronization, the vortex structure in the downstream wake is forced to reorganize and the hairpin-shape structure has a tendency to be well resumed.

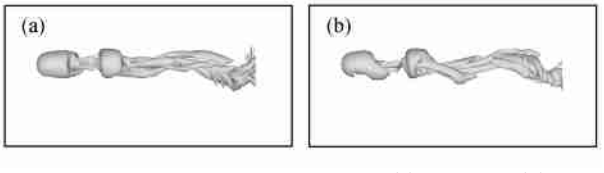

Fig. 10. Wake structure for $L/D=4.0$. (a) x-y view; (b) x-z view.

As the large gap 5.0 is reached, regular hairpin-shape structures are shed from the downstream sphere as well as the upstream sphere, and the symmetry is resumed now in the plane as mentioned above (Fig. 11).

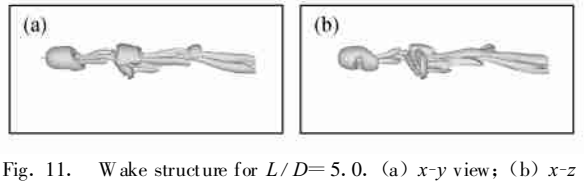

Fig. 11. Wake structure for $L/D=5.0$. (a) x-y view; (b) x-z view.

5 Conclusion

In this paper, the virtual boundary method provided by Goldstein is modified slightly and the computational performance has a distinct improvement. The modified method is extended to a 3D application and the flow field of two spheres in tandem arrangement at different gaps is investigated. Due to the interactions between two spheres, the flow regimes are found to be more complicated than that of a single sphere.

(i) At small gap ($\approx$1.5), due to the mutual suppress between the wakes of the two spheres, the full flow field is stable and axisymmetric.

(ii) At gap 2.0, an asymmetric but stable flow is constructed through a certain bifurcation. The downstream wake structure is characterized by a double-thread vortical structure that comprises two slender parallel vortex tubes. The double-thread structure has a planar symmetry.

(iii) At gap 2.5, the hairpin-shape vortices are periodically shed from the downstream sphere, but the planar symmetry remains.

(iv) The vortex structures at gaps ranging from 3.0 to 4.0 are irregular and a kind of 3D transition happens.

(v) At gap 5.0 the hairpin-shape structures are reconstructed behind the upstream and the downstream sphere and the planar symmetry is resumed.

Acknowledgement The authors would like to express their sincere thanks to the Center for Engineering and Scientific Computation of Zhejiang University for providing the SGI Origin3900 machine for all the computational tasks.

References

1 Taneda S. Experimental investigation of the wake behind a sphere at low Reynolds numbers. Journal of the Physical Society of Japan, 1956, 11(10): 1104—1108.
2 Magavery R. H. and Bishop R. L. Transition ranges for three-dimensional wakes. Canadian Journal of Physics, 1961, 39: 1418—1422.
3 Sakamoto H. and Haniu H. The formation mechanism and shedding frequency of vortices from a sphere in uniform shear flow. Journal of Fluid Mechanics, 1995, 287: 151—171.
4 Johnson T. A. and Patel V. C. Flow past a sphere up to a Reynolds number of 300. Journal of Fluid Mechanics, 1999, 378: 19—70.
5 Lee S. A numerical study of the unsteady wake behind a sphere in a uniform flow at moderate Reynolds numbers. Computers & Fluids, 2000, 29: 639—667.
6 Yutaka T., Yoshinobij M. and Kozo T. Fluid-dynamic interaction between two spheres. International Journal of Multiphase Flow, 1982, 8(1): 71—82.
7 Schouveiler L., Brydon A., Leweke T. et al. Interactions of the wakes of two spheres placed side by side. European Journal of Mechanics B/Fluids, 2004, 23: 137—145.
8 Kim I. and Elghobashi S. Three-dimensional flow over two spheres placed side by side. Journal of Fluid Mechanics, 1993, 246: 465—488.
9 Goldstein D., Handler R. and Sirovich L. Modeling a no-slip flow boundary with an external force field. Journal of Computational Physics, 1993, 105: 354—366.
10 Fadlun E. A., Verzicco R., Orlandi P. et al. Combined immersed-boundary finite-difference methods for three-dimensional complex flow simulations. Journal of Computational Physics, 2000, 161: 35—60.
11 Harlow F. H. and Welch J. E. Numerical calculation of time-dependent viscous incompressible flow of fluid with free surface. Physics of Fluids, 1965, 8(12): 2182—2189.
12 Abdallah S. Numerical solutions for the pressure poisson equation with Neumann boundary conditions using a non-staggered grid, I. Journal of Computational Physics, 1987, 79: 182—192.
13 Abdallah S. Numerical solutions for incompressible Navier-Stokes equations in primitive variables using a non-staggered grid, II. Journal of Computational Physics, 1987, 70: 193—202.
14 Jeong J. and Hussain F. On the identification of a vortex. Journal of Fluid Mechanics, 1995, 285: 69—94.